# Revealing the tunable photoluminescence properties of graphene quantum dots

Sk, Mahasin Alam; Ananthanarayanan, Arundithi; Huang, Lin; Lim, Kok Hwa; Chen, Peng

2014

https://hdl.handle.net/10356/101020

https://doi.org/10.1039/C4TC01191K

# Revealing the tunable photoluminescence properties of graphene quantum dots†

**Mahasin Alam Sk,[a] Arundithi Ananthanarayanan,[a] Lin Huang,[a] Kok-Hwa Lim,*[b] and Peng Chen*[a]**

[a]*Division of Bioengineering, School of Chemical and Biomedical Engineering, Nanyang Technological University, 70 Nanyang Drive, 637457, Singapore*
[b]*Singapore Institute of Technology, 10 Dover Drive, 138683, Singapore*

Graphene quantum dots (GQDs) are a new class of fluorescent reporters promising various novel applications including bio-imaging, optical sensing and photovoltaics. They have recently attracted enormous interest owing to their extraordinary and tunable optical, electrical, chemical and structural properties. The widespread use of GQDs, however, is hindered by the current poor understanding of their photoluminescence (PL) mechanisms. Using density-functional theory (DFT) and time-dependent DFT calculations, we reveal that the PL of a GQD can be sensitively tuned by its size, edge configuration, shape, attached chemical functionalities, heteroatom doping and defects. In addition, it is discovered that the PL of a large GQD consisting of heterogeneously hybridized carbon network is essentially determined by the embedded small $sp^2$ clusters isolated by $sp^3$ carbons. This study not only provides explanation to the previous experimental observations but also provides insightful guidance to develop methods for controllable synthesis and engineering of GQDs.

*Corresponding author emails: chenpeng@ntu.edu.sg or KokHwa.Lim@SingaporeTech.edu.sg
† Electronic Supplementary Information (ESI) available: computational methods, calculated ground-state band gap, emission wavelength and energy; structures and molecular orbitals of GQDs

Graphene is a single-atom-thin two-dimensional sheet consisting of hexagonally-packed carbon atoms (or a giant polycyclic aromatic molecule from chemist's point of view). It has been recently discovered that, when graphene shrinks to zero-dimension (nanoscale lateral dimensions), it fluoresces.[1-2] These so-called graphene quantum dots (GQDs) have quickly received much attention due to their unique structural and optoelectronic properties, and their great potentials in various applications such as bio-imaging[3-10] and display, photovoltaics,[11-12] energy storage,[13] and sensing.[14-15] Particularly, these glowing carbon nano-crystals can serve as new guiding lights for cell biologists. As we have shown recently, GQDs can be employed as the universal fluorescent tags to specifically label the molecular targets and enable real-time imaging of their trafficking dynamics in live cells.[7] GQDs are expected to outperform the current fluorescent reporters (fluorescent proteins, organic dyes, and semiconductor quantum dots) in many applications because of the unique combination of several key merits including tunable photoluminescence (PL) properties, excellent photo-stability, bio-compatibility, molecular size, and ease to be chemically paired with any biomolecule without compromising its functions.

The widespread use of GQDs, however, is currently hindered by the lack of controllable synthesis methods and the poor understanding of their tunable photoluminescence (PL) properties. Contradictory hypotheses sometimes arise from inconsistent experimental observations because of the large heterogeneity of GQDs synthesized by the current methods and the fact that the PL properties of GQDs are intriguingly determined by a number of parameters. Using density functional theory (DFT) and time-dependent density functional theory (TDDFT), we herein provide systematic theoretical investigations to show that the emission of GQDs can be widely tuned from deep ultraviolet to near infrared by its size, edge configuration, shape, functional groups, defects, and heterogeneous hybridization of carbon network.

Pristine graphene is known as a zero band gap material with infinite exciton Bohr radius due to the linear energy dispersion of the charge carriers.[16] Therefore, quantum confinement arises in a graphene sheet with finite size and becomes prominent in GQDs. Hence, band gap opening (and related PL emission) of GQD should be highly size-dependent, i.e., the larger its diameter the longer wavelength it emits. Such expected size-dependent emission, however, has not been unambiguously demonstrated experimentally. The synthesized GQDs (ranging from 1.5 to 60 nm) can emit different PL colors (including deep UV, blue, green, yellow and red) without obvious size dependence[1]. The large GQDs (~60 nm) synthesized by pyrolysis of hexa-*peri*-hexabenzocoronene (HBC) molecules emit blue fluorescence.[17] However, the small GQDs (1.5 – 5 nm) hydrothermally cropped from graphene oxide (GO) sheets are green fluorescent.[18] With similar size (2 – 3 nm), the GQDs oxidatively exfoliated from carbon black are green[7] while the GQDs electrochemically cut from defect-free CVD-grown graphene are blue.[15] These observed discrepancies are because of the large and uncontrolled heterogeneity of GQDs synthesized by the current approaches and the fact that the optical properties of GQDs sensitively depend on a number of parameters (e.g., size, chemical moieties, and defects). Theoretical modeling and calculations allow us to specifically investigate the influences of any particular parameter (computational methods are described in ESI).

To reveal the size-dependent PL of GQD, we calculated the emission wavelength of pristine zigzag-edged GQDs with different diameters (Fig. S1, ESI†). As shown in Fig. 1, these GQDs (G1- G6) fluoresce from deep UV to near infrared while varying the size from 0.46 to 2.31 nm. Specifically, the smallest GQD (benzene) emits at 235.2 nm while 2.31 nm GQD emits at 999.5 nm. The observed linear and steep size-dependence indicates that by varying the diameter of GQD from 0.89 to 1.80 nm its emission covers the entire visible light spectrum (400 - 770 nm).

The calculated emission wavelengths in vacuum (235.2, 399.5, 492.3 nm) of G1-G3 (defect- and functionality-free small $sp^2$-carbon clusters known as benzene, coronene, ovalene) correlates well with the experimental measurements (~278 nm in water,[19] ~427 nm in dimethyl sulphoxide,[20] ~484 nm in tetrabutylammonium sulfonate salt,[21] respectively). The red-shift of emission wavelength with increasing size is due to decrease of band gap resulting from π-electron delocalization (Table S1, ESI†). Similar size-dependent emission have also been observed in various spherical semi-conductor QDs [22-26]. But it is much more prominent in GQDs due to their small size.
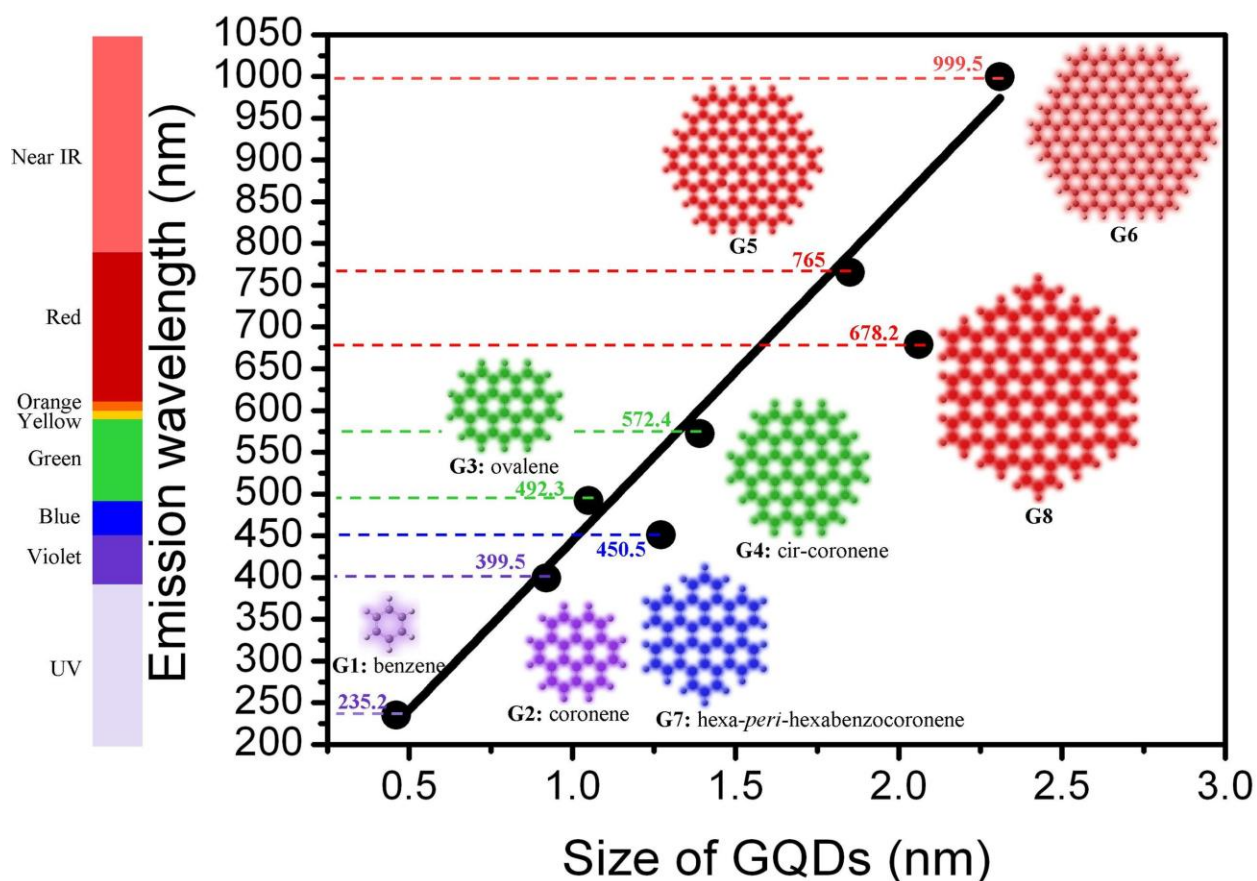
**Fig. 1** Calculated emission wavelength (nm) using TDDFT method in vacuum as a function of the diameter of GQDs. The solid line is the linear fitting of zigzag-edged GQDs (G1 – G6). The indicated diameter is the average of the horizontal and vertical dimensions.

Graphene can have either zigzag or armchair edges which exhibit distinct quantum confinement properties. It has been shown that graphene nanoribbons (GNRs) with dominant zigzag edges have a smaller band gap (0.14 eV) as compared to similarly-sized GNRs with dominant armchair edges (0.38 eV),[27] because of localized states on zigzag edges.[28] Consistently, we observe that the localized states in zigzag-edged GQD are pushed to the edge sites while similarly-sized armchair-edged GQD has localized states scattered in the center (Fig. S2, ESI†). Distinct to armchair-edged counterparts, the localized states at zigzag edge sites lower the energy of conduction band and thus reduce the band gap. Thus, it is expected that the armchair edge would widen the band gap of GQD and consequently blue-shift the emission. Indeed, our calculations show that 1.27 nm and 2.06 nm armchair-edged GQDs (G7 and G8 in Fig. 1) emit at 450.5 and 678.2 nm while the predicted emission wavelengths of their zigzag-edged counterparts are ~551 and ~872 nm, respectively.

As we have shown, the pristine GQD of ~2 nm in size is red-fluorescent. But most GQDs of similar size synthesized by top-down exfoliation of larger-sized carbon materials are green or blue,[7, 15, 18] presumably because of the disruption of the crystalline $sp^2$-hybridized carbon network of graphene caused by the exfoliation processes. Using a bottom-up strategy, a pristine armchair-edged GQD (consisting of 132 conjugated carbon atoms, approximately arranged in rectangle shape) has been synthesized by conjugating benzene derivatives (Fig. 2a, G9).[29] Such GQD (a polycyclic aromatic hydrocarbon) emits red fluorescence (670 nm) in toluene,[30] which is

close to our calculated emission wavelength of 667.4 nm in vacuum and calculation by Zhao et al[31]. The adsorption spectrum of this GQD peaks at ~535 nm attributed to the transition from ground-state $S_0$ to excited singlet state $S_3$ ($S_0{\rightarrow}S_3$).[30] Consistently, our calculations also predict the $S_0{\rightarrow}S_3$ transition at 542.96 nm. Another pristine armchair-edged GQD (Fig. 2b, G10: 168 carbons approximately arranged in triangle shape) synthesized by a bottom-up method shows the absorption maximum at ~591 nm[32]. Our calculated absorption peak in vacuum (594.6 nm) is in good agreement with the experimental observation and the values calculated by Zhao et al[31] and Schumacher.[33] We predict that this GQD emits red fluorescence at 747.0 nm which is consistent with the calculated emission wavelength of 748.60 nm in toluene by Zhao et al.[31]



**(a)**

Emission: 667.4 nm

**G9:** $C_{132}H_{38}$

**(b)**

Emission: 747.0 nm

**G10:** $C_{168}H_{42}$

**(c)**

Emission: 755.1 nm

**G11:** $C_{170}H_{42}$

**(d)**

Band gap: 0.19 eV

**G12:** $C_{100}H_{26}$

**(e)**

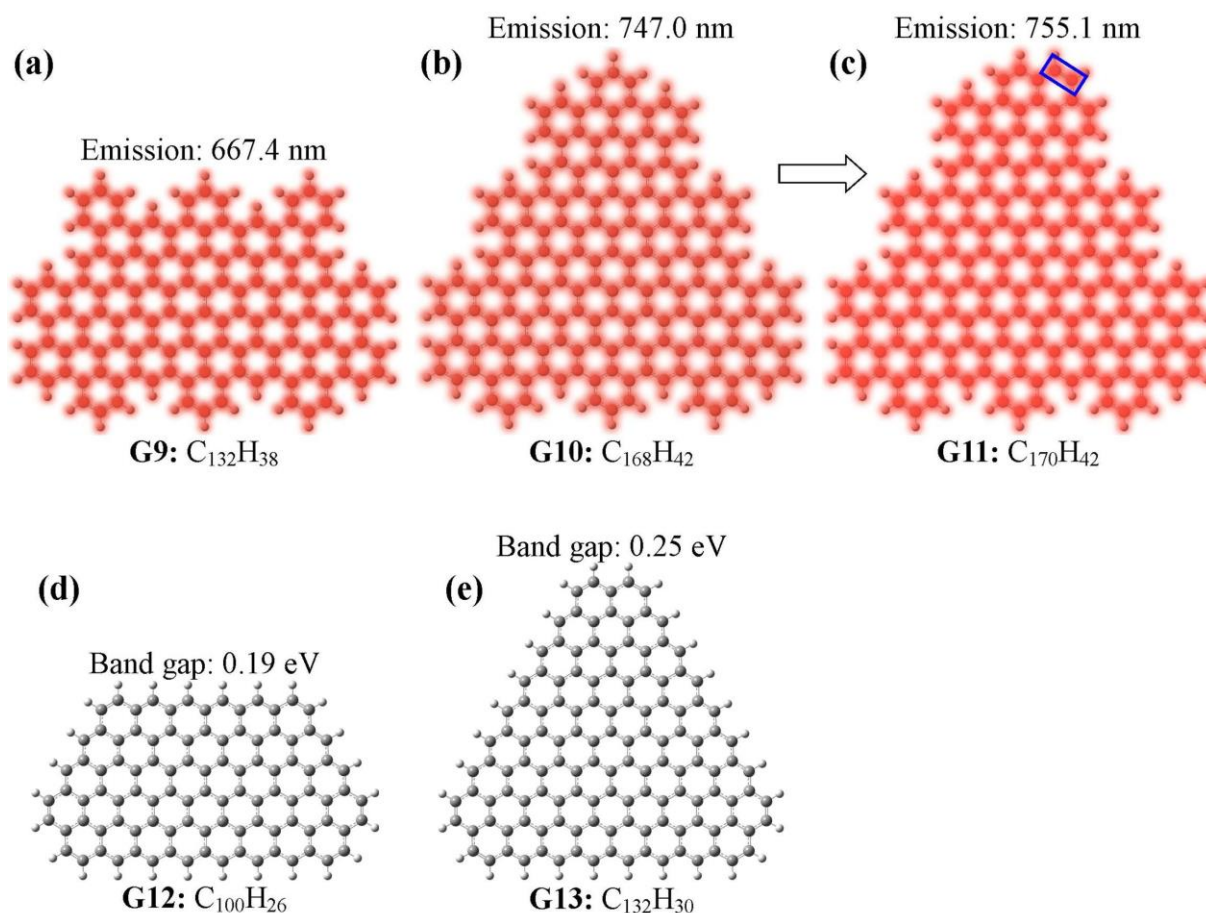Band gap: 0.25 eV

**G13:** $C_{132}H_{30}$

**Fig. 2** The structure of pristine (a) armchair-edged GQD ($C_{132}H_{38}$), (b) armchair-edged GQD ($C_{168}H_{42}$), (c) armchair-edged GQD ($C_{170}H_{42}$), formed by inserting two additional carbons (marked by blue rectangle) on $C_{168}H_{42}$ GQD, (d) zigzag-edged GQD ($C_{100}H_{256}$) and (e) zigzag-edged GQD ($C_{132}H_{30}$).

It is experimentally found that inserting two additional carbon atoms to create 6 zigzag edge sites on G10 (Fig. 2c, G11) red-shifts the absorption peak[29] from ~591 to ~604 nm which perfectly matches with our calculated value of 603.86 nm. We attribute this red-shift to band gap reduction of 0.06 eV. We also predict that G11 (Fig. 2c) emits red fluorescence at 755.1 nm which agrees with the calculation by Zhao et al.[31] Furthermore, we find that transforming G9 and G10 to zigzag-edged by removing some carbon atoms at the edges (G12, G13 in Fig. 2d and e) renders them non-fluorescent because of large reduction of band gap (from 2.34 to 0.19 eV, 2.14 to 0.25 eV, respectively). Clearly, optoelectronic properties of GQDs are highly sensitive to the edge configurations. Moreover, hexagonal zigzag-edged GQDs (G5 with 96 carbons and G6 with 150 carbons) exhibit much larger band gap as compared with similarly-sized and also zigzag-edged G12 (100 carbons arranged in rectangle shape) and G13 (132 carbons and triangle shape). Evidently, in addition to size and edge configuration, shape also plays an important role in determining the optoelectronic properties of GQDs.

The synthesized GQDs often bear functional groups (e.g., oxygenated groups resulting from the oxidative exfoliation processes). We show here that oxidation of GQDs by –OH or –COOH functional groups red-shifts the emission peaks due to band gap reduction, in a coverage dependent manner (Fig. 3a). Attaching –OH groups to the edge carbon atoms (varying from 0 - 100% coverage) continuously tunes G4 from green (572.4 nm) to red (732.3 nm). Edged -COOH

groups also red-shift the fluorescence emission (Fig. 3a). Compared to the edge functionalization, -OH groups conjugated on the basal plane of GQD cause more drastic red-shift because of disruption of graphitic carbon lattice. Specifically, two -OH groups on the basal plane of G4 makes it to emit red fluorescence at 746.1 nm. The predicted red-shift of oxidized GQDs is in line with experimental observations. For example, the GQDs (2-7 nm) exfoliated by acid oxidation emit greenish yellow-luminescence (~500 nm) and they become blue-luminescence (~450 nm) after reduction by $NaBH_4$.[34] GQDs synthesized by top-down methods usually bear defects. Our calculations show that creating single or double vacancy defects on green G4 largely red-shifts the emission peak to 1787.3 or 1217.0 nm, respectively (Fig. 3b and c). It indicates the strong influence of vacancy defects.
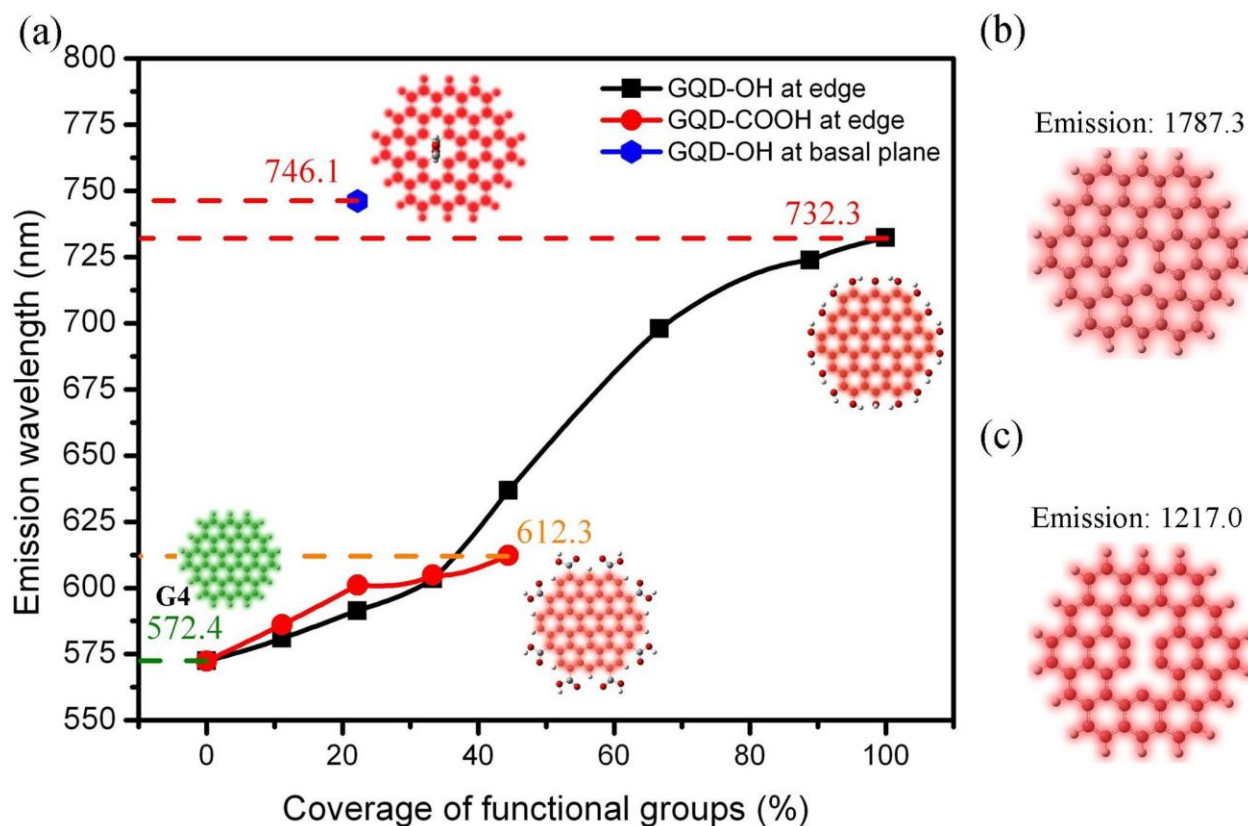


**Fig. 3** (a) Emission wavelength of oxidized GQD (G4) as a function of the coverage of –OH and –COOH groups. (b) and (c) are G4 with single or double vacancy defect, respectively.

Heteroatom doping is another way to alter the optoelectronic properties of graphene materials.[35] For example, it has been shown by Li et al that nitrogen-doping (with pyridinic and pyrrolic N atoms; N/C atomic ratio of ca. 4.3%) causes blue-shift of GQD emission.[36,11]. To understand this phenomenon, we investigate the effects of three different N-doping configurations (graphitic, pyridinic, and pyrrolic). Graphitic N-doping (at edge or center) on the green G4 GQD drastically lowers the band gap, thus rendering it non-fluorescent (Fig. 4a). In contrast, graphitic N-doping in large graphene sheet opens band gap near Dirac point by suppressing the density of state.[35,37] On the other hand, pyridinic N-doping on GQD causes slight blue-shift in a concentration dependent manner (i.e., 12.5 at% N-doping shifts the G4 emission from 572.4 to 550.3 nm) (Fig. 4b). Pyrrolic N-doping usually forms at the edged five-membered rings of GQD. To simulate its effect, we modify G4 GQD by attaching six cyclopentadiene at the edges. The resultant N-free GQD emits red fluorescence at 624.4 nm (Fig. 4c). It is observed that introduction of pyrrolic N atoms at the edges significantly blue-shifts the emission in a concentration dependent manner. Specifically, 9.09 at% pyrrolic N-doping transforms the red GQD to green (emission at 575.5 nm). Our calculations suggest that the blue-shift observed by Li et al is mainly due to pyrrolic N-doping.

Thus far, we have demonstrated that the PL properties of GQDs can be widely tuned by their size, edge structure, shape, functional groups, defects, and heteroatom doping. However, red-shifting effects induced by functional groups and defects cannot explain why relatively large and dopant-free GQDs (a few nm) synthesized by top-down methods are usually green or blue, instead of red as predicted in Fig. 1.[7, 15, 18] Loh et al. ,[38] Chien et al.[39] and Eda et al.[40] have proposed that the small $sp^2$ clusters isolated within the $sp^3$ carbon network are responsible for PL

emission arisen from graphene oxide (GO) sheets. We speculate that, just like GO, most synthesized GQDs are composed of isolated $sp^2$ clusters which dictate the PL properties of GQD.
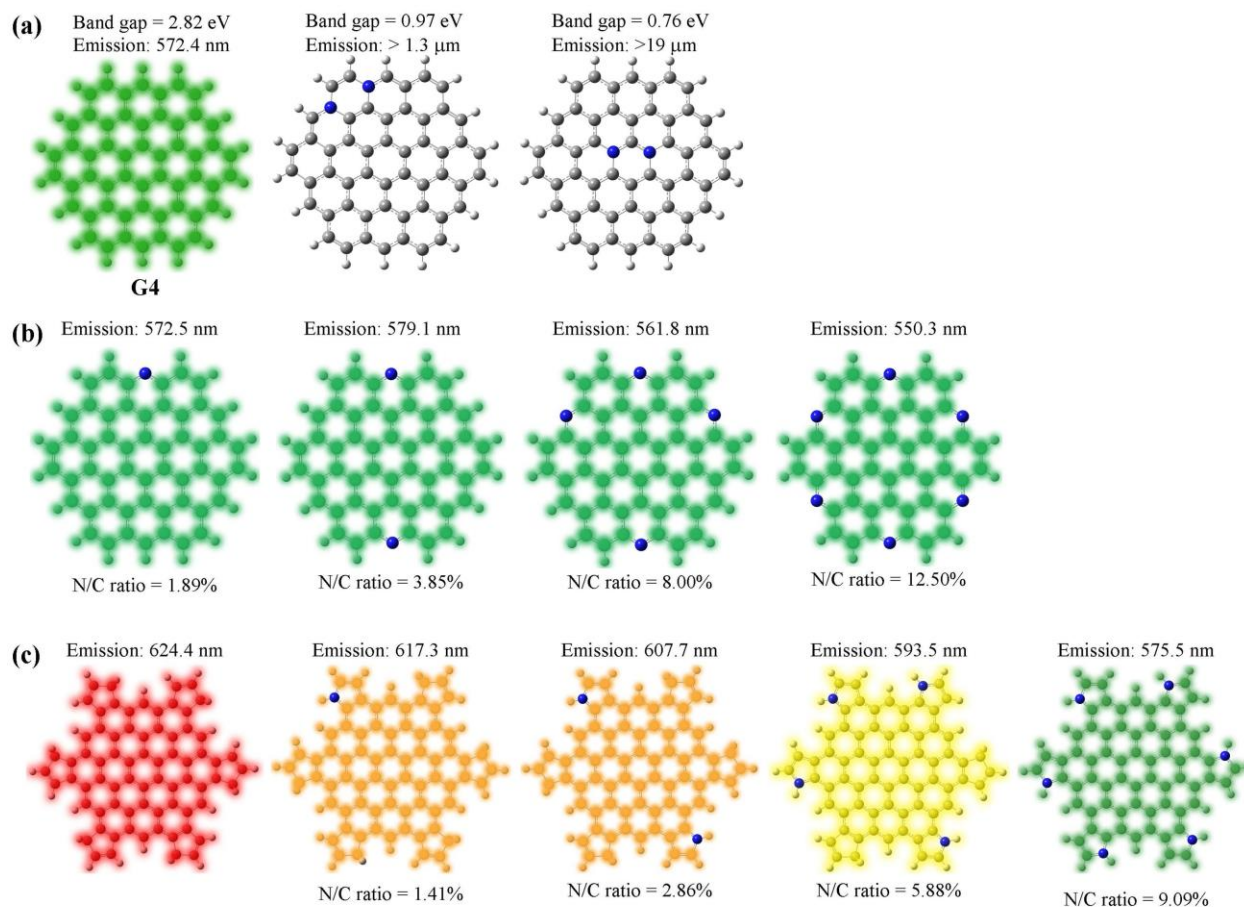


**Fig. 4** N-doped GQDs with (a) graphitic, (b) pyridine-like and (c) pyrrolic nitrogen. Blue spheres represent N atoms.

To test this hypothesis, we calculated the emission of molecular models consisting of small $sp^2$ clusters (benzene or coronene) joined by either $sp^2$ or $sp^3$ carbons (Fig. 5). Our calculations show that the molecule consisting of two benzene molecules connected *via* two $sp^2$ carbons (i.e., anthracene molecule, Fig. 5a) emits blue fluorescence at 435.0 nm (similar to the experimental measurement[19]) whereas the molecule emits DUV at 256.9 nm or 241.9 nm when the benzene

10

rings are connected with two (Fig. 5b) and six (Fig. 5c, top) sp$^3$ carbons, respectively. Similarly, when six benzenes and two coronenes are joined by sp$^3$ carbons, the emission of the entire GQD is close to individual benzene or coronene molecules (Fig. 5d-g). These results imply that, when small sp$^2$ clusters are isolated by sp$^3$ carbons, $\pi$-electrons are confined within these domains and PL emission is dominated by these small individual clusters.

To investigate the effects of oxidation, two –OH groups are attached to benzene without altering the sp$^2$ hybridization state of carbon atoms. This shifts the emission wavelength from 241.9 to 274.5 nm (Fig. 5c, middle). On the other hand, attaching two –OH groups onto the bridging sp$^3$ carbons only slightly shifts the emission to 248.8 nm (Fig. 5c, bottom). This suggests that oxidation at sp$^2$ clusters can exert stronger influence than oxidation at sp$^3$ carbons.

Fig. 6a depicts a GQD ($C_{96}H_{58}$) consisting of 4 sp$^2$ domains (pyrene) separated by sp$^3$ carbon network. This GQD has a ground-state band gap of 3.58 eV, which is much larger than that of the pristine sp$^2$-hybridized counterpart (0.35 eV). It emits violet fluorescence at 418.1 nm which is red-shifted as compared to free pyrene molecule (emitting at 359.4 nm). The pyrene domains embedded in $C_{96}H_{58}$ GQD are bonded to either (a) five sp$^3$ carbons (pentamethyl pyrene which emits at 389.2 nm) or (b) six sp$^3$ carbons (hexamethyl-pyrene which emits at 404.9 nm) (Fig. 6a). Evidently, the emission of the entire GQD is dependent more strongly on the hexamethyl-pyrene domains.
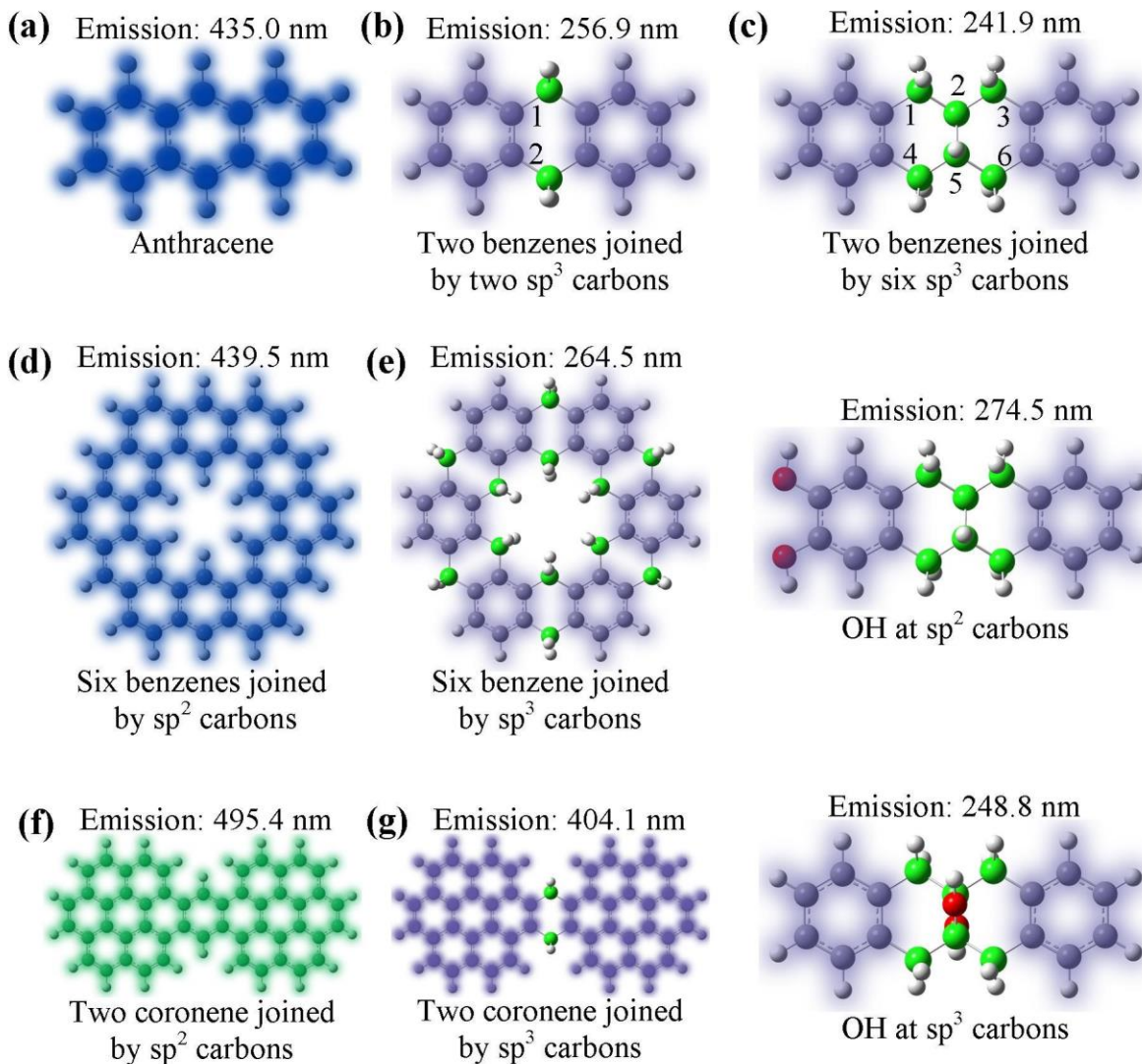
**Fig. 5** Two benzenes joined *via* (a) two sp$^2$ carbons (i.e., anthracene), (b) two sp$^3$ carbons (green spheres), or (c) six sp$^3$ carbons (top). In c, middle: two H atoms of benzene are substituted with –OH groups (red spheres); bottom: substituting two H atoms of the bridging sp$^3$ carbons with –OH groups. (d and e) Six benzenes are joined *via* sp$^2$ or sp$^3$ carbons, respectively. (f and g) Two coronenes are joined *via* sp$^2$ or sp$^3$ carbons, respectively.
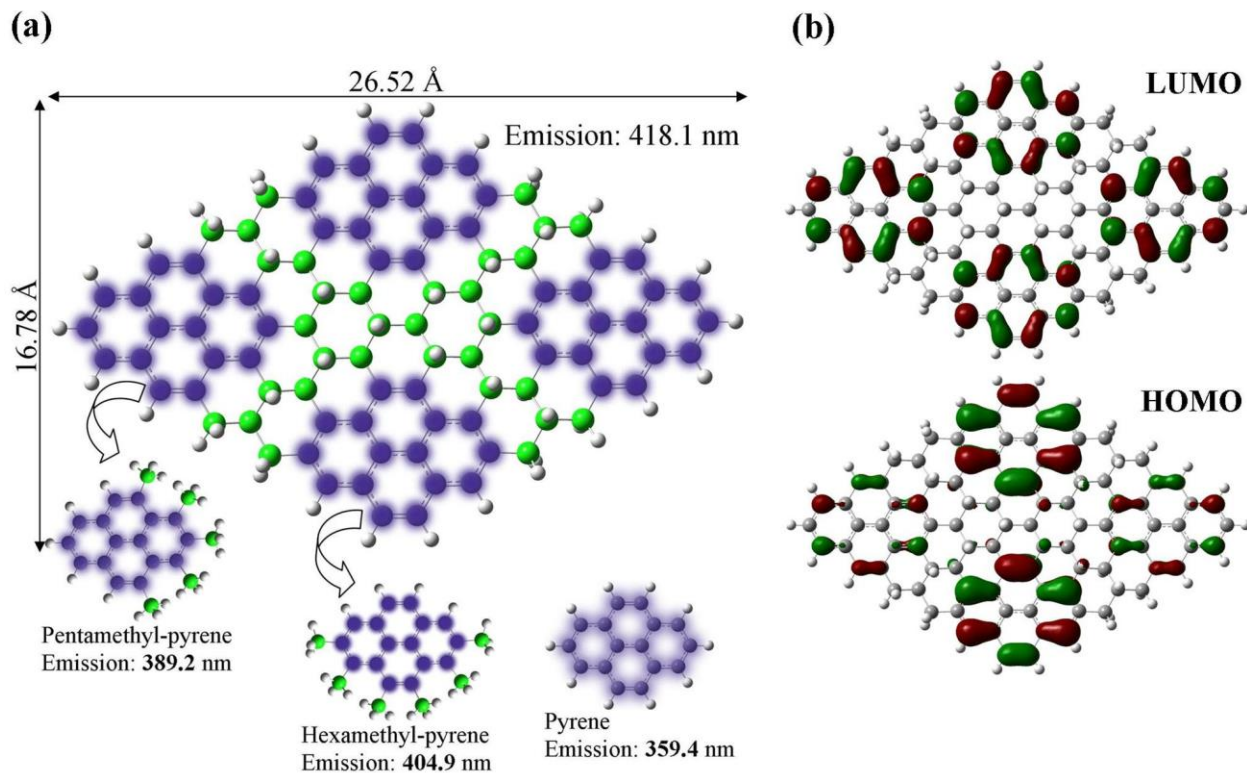
**Fig. 6** (a) GQD composed of four pyrene domains separated by sp$^3$ carbons (green spheres). (b) Molecular orbitals for LUMO and HOMO from ground-state.

The major electronic transition causing GQD emission is from the lowest unoccupied molecular orbital (LUMO) to highest occupied molecular orbital (HOMO) (~95% for $C_{96}H_{58}$ GQD). Molecular orbitals for the LUMO and HOMO reveal that PL emission arises from the pyrene domains, and the molecular orbitals of HOMO are mainly from the hexamethyl-pyrene domains (Fig. 6b). Therefore, it can be concluded that PL of a heterogeneous GQD ($C_{96}H_{58}$ here) is essentially determined by its sp$^2$ domains of lowest energy band gap (hexamethyl-pyrene here). To further support the notion that the PL properties of heterogeneously hybridized GQDs are dictated by the small sp$^2$ clusters, we show that increasing the size of sp$^2$ domains leads to the decrease of ground-state band gap of GQD (Fig. S3, ESI†). In addition, with the size of sp$^2$

clusters fixed, increasing the diameter of GQDs (as well as the number of $sp^2$ clusters) does not alter the ground-state band gap (Fig. S4, ESI†).

This study provides explanation to the previous experimental observations. For example, the peculiar size-increase induced blue-shift observed by Kim et al. can be explained by the increase of armchair edge configurations in large GQDs.[41] Hexa-peri-hexabenzocoronene (HBC) emits blue fluorescence at ~490 nm in 2-methyl-tetrahydrofuran.[42] GQDs (~60 nm) obtained by pyrolysis of HBC molecules followed by oxidative exfoliation also fluoresce similarly (~489 nm) .[17] Thus, it is conceivable that the HBC domains in such a large GQD are connected by $sp^3$ carbons causing π-electrons to localize on the $sp^2$ hybridized HBC domains. Gokus et al. have shown that PL can be induced in graphene by oxygen plasma treatment and attributed this phenomenon to CO-related localized electronic states at the oxidation sites but not to $sp^2$ sites.[43] But, we show that oxygenated functional groups can only lower the band gap (instead of opening band gap for PL emission). Therefore, their observation should be resulted from creation of small $sp^2$ clusters on graphene sheet. The GQDs synthesized from top-down approaches exhibit excitation-dependent behavior and broad emission spectrum.[11-12, 15, 17, 44-45] This can be attributed to the heterogeneity of produced GQDs in size, shape, functional groups, defects, and composition of $sp^2$ clusters.

In summary, we for the first time have systematically studied the mechanisms underlying the tunable PL properties of GQDs using DFT and TDDFT calculations. It is revealed that the emission of zigzag-edged pristine GQDs can cover the entire visible light spectrum by varying the diameter from 0.89 to 1.80 nm. Armchair edge and pyrrolic N-doping blue-shift the GQD PL emission whereas chemical functionalities and defects cause red-shift. The PL emission of a heterogeneously hybridized GQD is dictated by its isolated small $sp^2$ domains. As shown, GQDs

can be tailored to emit a wide range of wavelengths. This study confirms the exciting possibility of GQDs to serve as universal fluorophores for various imaging purposes and shall provide important insights and guidance for the development of methods to controllably synthesize GQDs with well-defined and desired properties towards specific purposes.

## Acknowledgements

# Notes and references

1. L. Li, G. Wu, G. Yang, J. Peng, J. Zhao and J.-J. Zhu, *Nanoscale*, 2013, 5, 4015-4039.
2. L. Lin, M. Rong, F. Luo, D. Chen, Y. Wanga and X. Chen, *Trends Anal. Chem.*, 2014, 54, 83-102.
3. Y. Dong, C. Chen, X. Zheng, L. Gao, Z. Cui, H. Yang, C. Guo, Y. Chi and C. M. Li, *J. Mater. Chem.*, 2012, 22, 8764-8766.
4. L. Zhang, Y. Xing, N. He, Y. Zhang, Z. Lu, J. Zhang and Z. Zhang, *J. Nanosci. Nanotechnol.*, 2012, 12, 2924-2928.
5. Q. Liu, B. Guo, Z. Rao, B. Zhang and J. R. Gong, *Nano letters*, 2013, 13, 2436-2441.
6. W. J. Xie, Y. Y. Fu, H. Ma, M. Zhang and L. Z. Fan, *Acta Chimica Sinica*, 2012, 70, 2169-2172.
7. X. T. Zheng, A. Than, A. Ananthanaraya, D.-H. Kim and P. Chen, *ACS Nano*, 2013, 7, 6278-6286.
8. M. M. Xie, Y. J. Su, X. N. Lu, Y. Z. Zhang, Z. Yang and Y. F. Zhang, *Mater Lett*, 2013, 93, 161-164.
9. Abdullah-Al-Nahain, J. E. Lee, I. In, H. Lee, K. D. Lee, J. H. Jeong and S. Y. Park, *Mol. Pharmaceut.*, 2013, 10, 3736-3744.
10. X. Wu, F. Tian, W. X. Wang, J. Chen, M. Wu and J. X. Zhao, *J Mater Chem C*, 2013, 1, 4676-4684.
11. Y. Li, Y. Hu, Y. Zhao, G. Shi, L. Deng, Y. Hou and L. Qu, *Adv. Mater.*, 2011, 23, 776-780.
12. V. Gupta, N. Chaudhary, R. Srivastava, G. D. Sharma, R. Bhardwaj and S. Chand, *J Am Chem Soc*, 2011, 133, 9960-9963.
13. W.-W. Liu, Y.-Q. Feng, X.-B. Yan, J.-T. Chen and Q.-J. Xue, *Adv. Funct. Mater.*, 2013, 23, 4111-4122.
14. H. Sun, L. Wu, W. Wei and X. Qu, *Mater. Today*, 2013, 16, 433-442.
15. A. Ananthanarayanan, X. Wang, P. Routh, B. Sana, S. Lim, D.-H. Kim, K.-H. Lim, J. Li and P. Chen, *Adv. Funct. Mater.*, 2014, 24, 3021-3026.
16. A. K. Geim and K. S. Nonoselov, *Nat. Mater.*, 2007, 6, 183-191.
17. R. Liu, D. Wu, X. Feng and K. Mullen, *J. Am. Chem. Soc.*, 2011, 133, 15221-15223.
18. D. Pan, L. Guo, J. Zhang, C. Xi, Q. Xue, H. Huang, J. Li, Z. Zhang, W. Yu, Z. Chen, Z. Li and M. Wu, *J. Mater. Chem.*, 2012, 22, 3314-3318.
19. F. P. Schwarz and S. P. Wasik, *Anal. Chem.*, 1976, 48, 524-528.
20. R. Waris, M. A. Rembert, D. M. Sellers, J. William E. Acree and J. Kenneth W. Street, *Analyst*, 1989, 114, 195-199.
21. S. A. Tucker, J. William E. Acree, J. Kenneth W. Street and J. C. Fetzer, *Appl. Spectrosc.*, 1989, 43, 162-164.
22. L. Zhang, L. Yin, C. Wang, N. lun, Y. Qi and D. Xiang, *J. Phys. Chem. C*, 2010, 114, 9651-9658.
23. H.-M. Cheng, K.-F. Lin, H.-C. Hsu and W.-F. Hsieh, *Appl. Phys. Lett.*, 2006, 88, 261909.
24. R. E. Bailey and S. Nie, *J. Am. Chem. Soc.*, 2003, 125, 7100-7106.
25. A. L. Efros, M. Rosen, M. Kuno, M. Nirmal, D. J. Norris and M. Bawendi, *Phys. Rev. B*, 1996, 54, 4843-4856.
26. E. Pedrueza, A. Segura, R. Abargues, J. B. Bailach, J. C. Chervin and J. P. Martínez-Pastor, *Nanotech*, 2013, 24, 205701.

27.  K. A. Ritter and J. Lyding, *Nat. Mater.*, 2009, 8, 235-242.
28.  K. Nakada, M. Fujita, G. Dresselhaus and M. S. Dresselhaus, *Phys. Rev. B*, 1996, 54, 17954-17961.
29.  X. Yan, X. Cui and L.-s. Li, *J. Am. Chem. Soc.*, 2010, 132, 5944-5945.
30.  M. L. Mueller, X. Yan, J. A. McGuire and L.-s. Li, *Nano Lett.*, 2010, 10, 2679-2682.
31.  M. Zhao, F. Yang, Y. Xue, D. Xiao and Y. Guo, *ChemPhysChem*, 2014, 15, 950-957.
32.  X. Yan, X. Cui, B. Li and L.-s. Li, *Nano Lett.*, 2010, 10, 1869-1873.
33.  S. Schumacher, *Phys. Rev. B*, 2011, 83, 081417.
34.  L.-L. Li, J. Ji, R. Fei, C.-Z. Wang, Q. Lu, J.-R. Zhang, L.-P. Jiang and J.-J. Zhu, *Adv. Funct. Mater.*, 2012, 22, 2971-2979.
35.  X. Wang, G. Sun, P. Routh, D.-H. Kim, W. Huang and P. Chen, *Chem. Soc. Rev.*, 2014, DOI: 10.1039/C1034CS00141A.
36.  Y. Li, Y. Zhao, H. Cheng, Y. Hu, G. Shi, L. Dai and L. Qu, *J. Am. Chem.Soc.*, 2012, 134, 15-18.
37.  D. Usachov, O. Vilkov, A. Gruneis, D. Haberer, A. Fedorov, V. K. Adamchuk, A. B. Preobrajenski, P. Dudin, A. Barinov, M. Oehzelt, C. Laubschat and D. V. Vyalikh, *Nano Lett.*, 2011, 11, 5401-5407.
38.  K. P. Loh, Q. Bao, G. Eda and M. Chhowalla, *Nature Chem.*, 2010, 2, 1015-1024.
39.  C.-T. Chien, S.-S. Li, W.-J. Lai, Y.-C. Yeh, H.-A. Chen, I.-S. Chen, L.-C. Chen, K.-H. Chen, T. Nemoto, S. Isoda, M. Chen, T. Fujita, G. Eda, H. Yamaguchi, M. Chhowalla and C.-W. Chen, *Angew. Chem., Int. Ed.*, 2012, 51, 6662-6666.
40.  G. Eda, Y.-Y. Lin, C. Mattevi, H. Yamaguchi, H.-A. Chen, I.-S. Chen, C.-W. Chen and M. Chhowalla, *Adv. Mater.*, 2010, 22, 505-509.
41.  S. Kim, S. W. Hwang, M.-K. Kim, D. Y. Shin, D. H. Shin, C. O. Kim, S. B. Yang, J. H. Park, E. Hwang, S.-H. Choi, G. Ko, Sunghyun Sim, C. Sone, H. J. Choi, S. Bae and B. H. Hong, *ACS Nano*, 2012, 6, 8203-8208.
42.  Bassem El Hamaoui, F. e. e. Laquai, S. Baluschev, J. Wu and K. M˙ullen, *Synthetic Metals*, 2006, 156, 1182-1186.
43.  T. Gokus, R. R. Nair, A. Bonetti, M. B. hmler, A. Lombardo, K. S. Novoselov, A. K. Geim, A. C. Ferrari and A. Hartschuh, *ACS Nano*, 2009, 3, 3963-3968.
44.  J. Shen, Y. Zhu, C. Chen, X. Yang and C. Li, *Chem. Comm.*, 2011, 47, 2580-2582.
45.  D. Pan, J. Zhang, Z. Li and M. Wu, *Adv. Mater.*, 2010, 22, 734-738.